Received: 16 July 2020 | Revised: 22 October 2020 | Accepted: 28 October 2020

DOI: 10.1002/aoc.6091

Applied Organometallic Chemistry WILEY

FULL PAPER

Magnetically recoverable copper ferrite catalyzed cascade synthesis of 1,3-dimethyl-6-nitro-5-arylpyrido[2,3-*d*]pyrimidine-2,4(1*H*,3*H*)-diones under microwave irradiation and solvent-less condition

Amar Jyoti Bhuyan[1] | **Pubanita Bhuyan**[1] | **Bornali Boruah**[2] | **Lakhinath Saikia**[1]

[1]Department of Chemistry, Rajiv Gandhi University (A Central University), Doimukh, India

[2]Department of Chemistry, Assam Down Town University, Guwahati, India

Correspondence
Lakhinath Saikia, Department of Chemistry, Rajiv Gandhi University (A Central University), Rono-Hills, Doimukh, Arunachal Pradesh 791112, India.
Email: lakhinath.saikia@rgu.ac.in

Funding information
Science and Engineering Research Board; DST-INSPIRE fellowship, Grant/Award Number: IF170498; Council of Scientific and Industrial Research (CSIR), India, Grant/Award Number: 02(0280)/16/EMR-II; Department of Science and Technology-Science and Engineering Research Board, India, Grant/Award Number: EMR/2016/003126

In recent years, magnetically active $CuFe_2O_4$ nanoparticles have been gaining significant interest in the field of heterogeneous catalysis as those can be easily prepared and effortlessly recovered from a reaction system. Here, we are reporting our work on cascade syntheses of 1,3-dimethyl-6-nitro-5-arylpyrido[2,3-*d*]pyrimidine-2,4(1*H*,3*H*)-diones starting from 6-[(dimethylamino)methylene-amino]-1,3-dimethyluracil, aromatic aldehydes and nitromethane using magnetically active $CuFe_2O_4$ catalyst system under microwave irradiation and solvent-less condition. The current methodology is a valued addition to the existing procedures of 5-arylpyrido[2,3-*d*]pyrimidines syntheses making best use of the diene behavior of 6-[(dimethylamino)methylene-amino]-1,3-dimethyluracil. However, heterogeneous catalysis has been employed for the first time to do the syntheses by carrying out [4 + 2]cycloaddition reaction between 6-[(dimethylamino)methylene-amino]-1,3-dimethyluracil and in situ generated 2-(2-nitrovinyl)arenes/heteroarenes. The methodology is highly time-economic, and along with other features like easy recovery and good reusability of the catalyst, simple operating procedure, wide substrate scope, and good to excellent product yield, it offers the chemists a reaction protocol worth trying for the syntheses of 1,3-dimethyl-6-nitro-5-arylpyrido[2,3-*d*]pyrimidine-2,4(1*H*,3*H*)-diones. While laboratory prepared catalyst system was characterized using FT-IR, XRD, SEM-EDX, VSM, XPS and TEM analysis, all the synthesized compounds have been characterized using ^{1}H and ^{13}C NMR spectroscopy and HRMS.

KEYWORDS

[4 + 2]cycloaddition reaction, 5-arylpyrido[2,3-*d*]pyrimidine, cascade synthesis, copper ferrite, magnetic nanoparticles

1 | INTRODUCTION

Research works toward construction of heterocyclic frameworks have always been constituting a pivotal area of research, as advancement of medicinal chemistry is considerably dependent on the development of newer and efficient synthetic methodologies for these heterocycles. Among various heterocycles, pyrido[2,3-*d*]pyrimidine is one of the most significant entities as numerous molecules bearing this core structure are established to have excellent biological activities like antitumor,[1–5] antitmicrobial,[6–11] anti-inflammatory,[12,13] herbicidal,[14] tyrosine kinase inhibitory activity,[15–18] and activity against dengue virus[19]. The moiety started gaining special attention from researchers dealing with antibacterial studies of synthesized compounds after the landmark publication by Stover et al. in Proceedings of the National Academy of Sciences of the United States of America.[20] They reported therein the screening of 1.6 million individual compounds from Pfizer compound library for antibacterial activity and identifying three pyrido[2,3-*d*]pyrimidine derivatives as potent synthetic antibacterial. The need of developing novel and efficient antibiotics to combat bacterial drug resistance along with broad spectrum of biological activities associated with pyrido[2,3-*d*]pyrimidine have made this unit a lucrative target for many synthetic chemists. So a plethora of reports have been found demonstrating efficient synthetic methodologies for organic molecules containing pyrido[2,3-*d*]pyrimidine core structure starting from a diverse set of substrates employing homogenous, heterogeneous, and catalyst-free procedures.[21–47] Among these, there are a good number of reports that describe excellent use of the diene nature of 6-[(dimethylamino) methylene-amino]-1,3-dimethyluracil (**1**) or related compounds to carry out [4 + 2] cycloaddition reactions with various electron deficient dienophiles for successful synthesis of pyrido[2,3-*d*]pyrimidine derivatives.[21–28] Although a few of these reports demonstrate multicomponent methodologies to carry out the transformation in or without presence of homogeneous catalyst,[21–23] not a single report has been found to employ heterogeneous catalyst system for the purpose.

In recent years, magnetically active $CuFe_2O_4$ particles have been widely and successfully used in many cascade synthetic processes.[48–52] We too developed a $CuFe_2O_4$ catalyzed rapid cascade synthetic methodology for 4-aryl-1*H*-1,2,3-triazoles starting from aromatic aldehydes, nitromethane, and NaN_3 under microwave irradiation.[53] In that line, we are reporting herein a $CuFe_2O_4$ catalyzed cascade methodology for the synthesis of 1,3-dimethyl-6-nitro-5-arylpyrido[2,3-*d*]pyrimidine-2,4(1*H*,3*H*)-diones (**4**) starting from 6-[(dimethylamino)methylene-amino]-1,3-dimethyluracil (**1**), aromatic aldehydes (**2**), and nitromethane (**3**) under microwave irradiation and solventless condition. The report is indeed first of its kind to adopt heterogeneous catalysis for cascade synthesis of 5-arylpyrido[2,3-*d*]pyrimidines involving [4 + 2]cycloaddition process and is a valued addition to the existing methodologies enabling significant minimization of time requirement as depicted in Scheme 1.

2 | RESULT AND DISCUSSION

2.1 | Catalyst preparation and characterization

$CuFe_2O_4$ catalyst system used for the purpose was prepared as discussed in our recent work by combined sonochemical and co-precipitation technique.[53] Characterization of the catalyst was done using electron dispersive X-ray (EDX) analysis, Fourier-transform-infrared spectroscopy (FT-IR), scanning electron microscopy (SEM), transmission electron microscopy (TEM), vibrating sample magnetometer (VSM) study, and X-ray photoelectron spectroscopy (XPS). SEM-EDX spectrum (Figure 1c) ascertains the elemental presence of Cu, Fe,

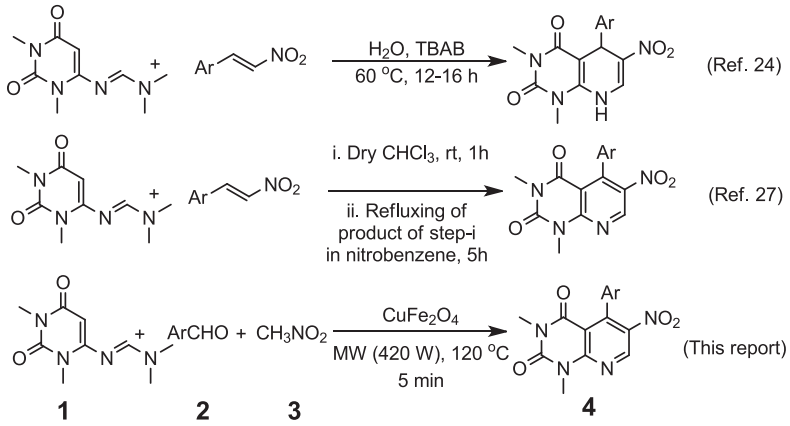

SCHEME 1 Comparison of reported and present work

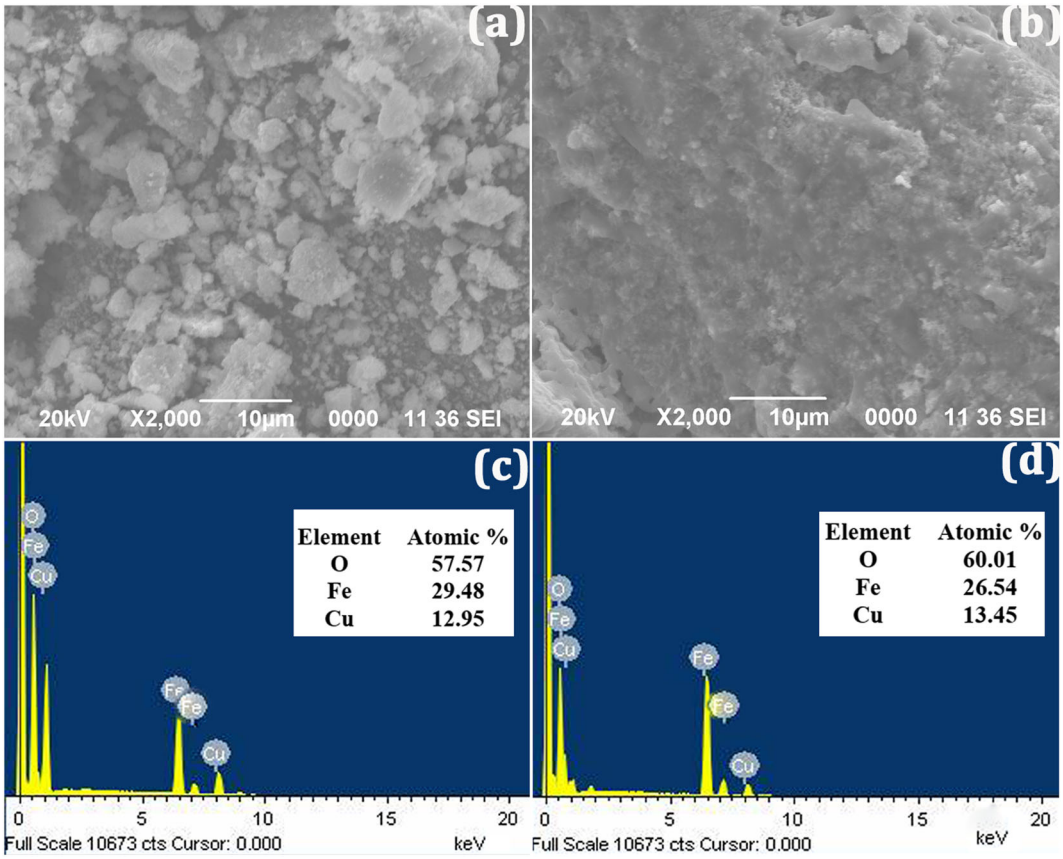

FIGURE 1 SEM images of fresh and recovered catalysts (a and b); EDX (SEM) spectra of fresh and recovered catalysts (c and d)

and O in 12.95, 29.48, and 57.57 atomic% respectively in the prepared sample. An absorption band at 581.10 cm^{-1} was observed in the FT-IR spectrum, which can be attributed to Fe—O stretching vibration (Figure 2).[48] Reflection peaks at 2θ values 18.2, 29.8, 35.3, 37.2, 42.8, 52.9, 56.5, and 62.3° were observed in XRD analysis (Figure 3), which are in good agreement with the characteristic peaks of tetragonal $CuFe_2O_4$ with good crystallinity.[49] From XRD data, average particle size was determined by using Scherrer equation $D = K\lambda/(d Cos\theta)$ and found to be 15.09 nm (calculation is shown in supporting information). Particle size of the nanoparticles was calculated from TEM image (Figure 4) too and found to be in the range of 13–18 nm, which is in good agreement with the size calculated using Scherrer equation. Coagulation of particles in the sample was unveiled by the TEM image (Figure 4a), which can be attributed to the magnetic nature of the particles. Diffraction spots were superimposed on the ring pattern (Figure 4b) in the selected area electron diffraction (SAED) analysis, which reveals polycrystalline nature of the material. Magnetic property of the prepared catalyst was analyzed by vibrating sample magnetometer under applied field of ±15 kOe at room temperature, the resulting hysteresis loop of which is shown in Figure 5. The three important parameters, namely coercivity, magnetization at saturation (Ms), and retentivity (Mr) of the sample were measured as 211.24 Oe, 32.390 emu/g and 6.5982 emu/g respectively from the hysteresis loop. The shape of the loop along

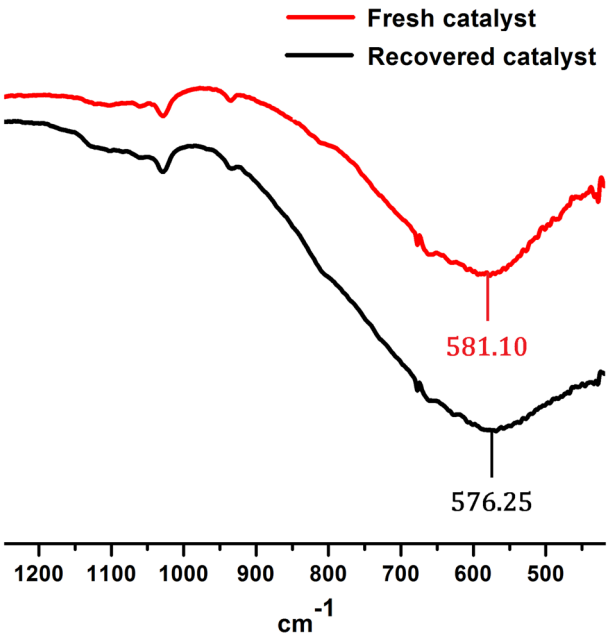

FIGURE 2 FT-IR spectra of the fresh and recovered catalyst

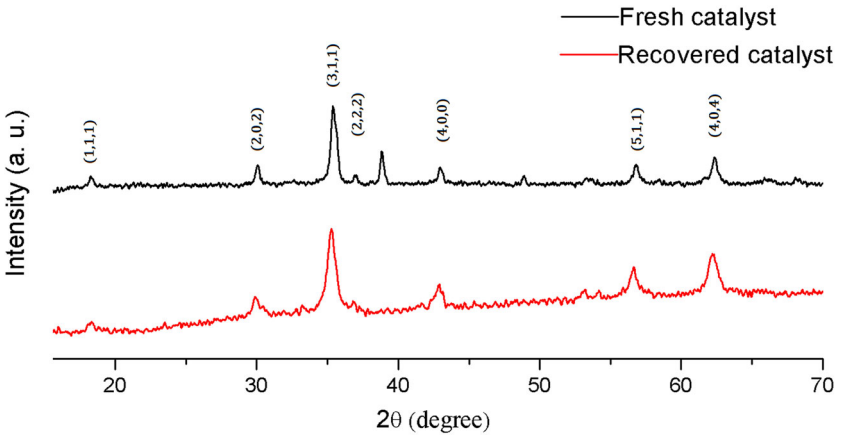

FIGURE 3 XRD spectra of fresh and recovered catalysts

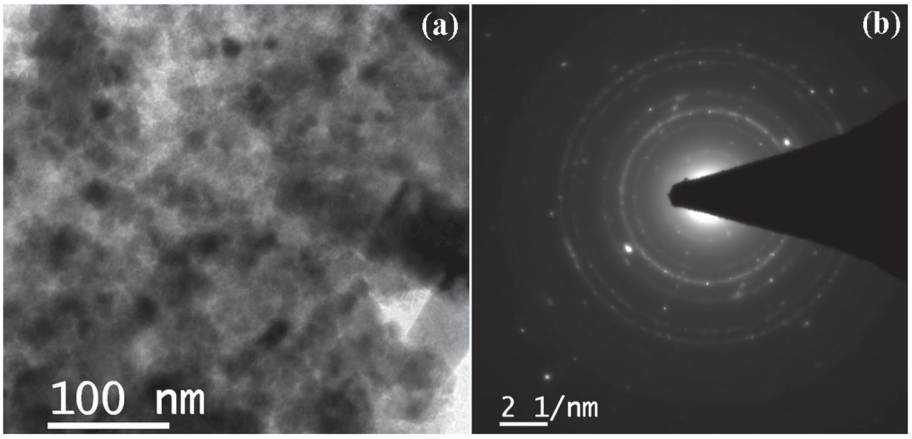

FIGURE 4 TEM and SAED images of $CuFe_2O_4$nanoparticles

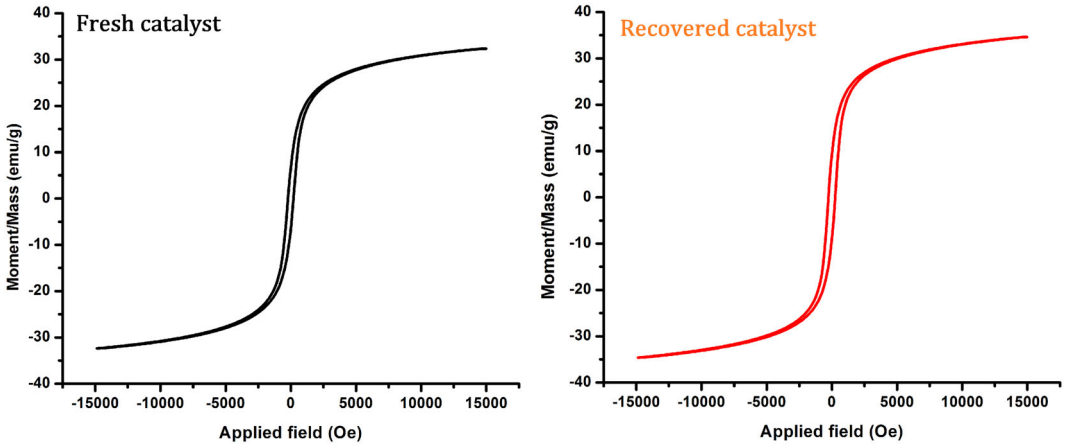

FIGURE 5 Hysteresis loop of fresh and recovered catalyst

with the value of magnetization at saturation (32.390 emu/g) reveal the ferromagnetic property of the material. XPS analysis was carried out to understand the chemical composition of the prepared sample. Charge correction of binding energies due to specimen charging was done by setting the binding energy of C 1 s at 284.6 eV. The survey spectrum as shown in Figure 6a clearly indicates the presence of Cu, Fe, and O in the sample. High resolution spectrum for Cu 2p showed a peak at 934.3 eV, which is characteristic of Cu $2p_{3/2}$ in $CuFe_2O_4$.[54] Peaks at binding energy values 942.8 and 954.4 eV correspond to Cu $2p_{3/2}$ satellite and Cu $2p_{1/2}$ peak respectively, confirming the presence Cu^{2+} in the sample (Figure 6b).[55,56] Fe 2p spectrum showed two

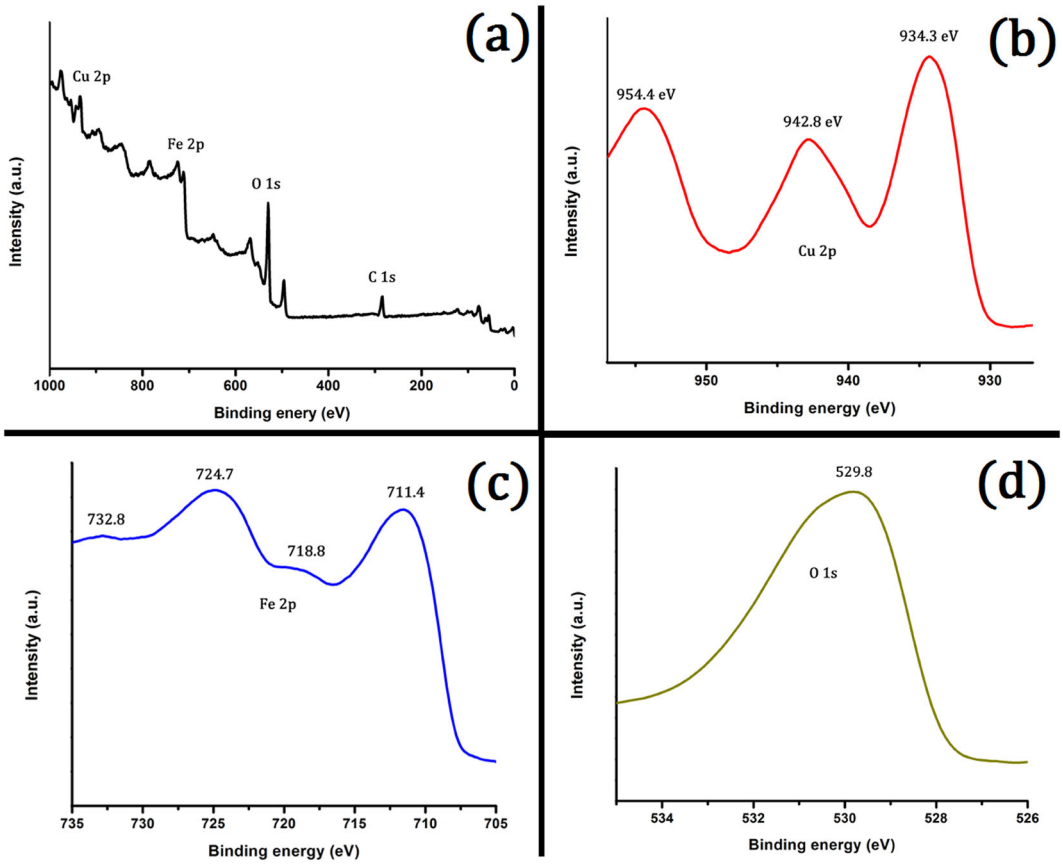

FIGURE 6 XPS spectrum of prepared $CuFe_2O_4$: Survey spectrum (a); high resolution spectrum of Cu 2p (b), Fe 2p (c) and O 1s (d)

major peaks at 711.4 and 724.7 eV, which correspond to Fe $2p_{3/2}$ and Fe $2p_{½}$ respectively.[55] Two accompanying satellite peaks at 711.4 and 732.8 in the spectrum indicate the presence of Fe in Fe^{3+} state (Figure 6c).[55] A peak centered at 529.8 eV was observed in the high resolution spectrum of O 1 s, which indicates the presence of O^{2-} (Figure 6d).[57] Elemental quantification from the peak area values of various peaks in the XPS spectrum showed the presence of Cu, Fe, and O in 13.82, 28.07, and 58.1 atomic%, respectively, which confirms that the prepared sample possesses an empirical formulae of $CuFe_2O_4$.

2.2 | Catalytic activity

To evaluate the catalytic activity of the prepared catalyst in multicomponent synthesis of **4** starting from **1**, aromatic aldehydes (**2**) and nitromethane (**3**), its catalytic activity was checked by carrying out a model reaction (Scheme 2) among **1**, *p*-nitrobenzaldehyde (**2a**), and nitromethane (**3**) under various reaction conditions and the results observed are summarized in Table 1. Both conventional and microwave heating (using a monomode microwave synthesizer by Raga's Scientific Microwave Synthesis System) were examined as source of energy for performing the reactions. Table 1 clearly reveals better outcome of the reactions under microwave irradiation over conventional heating. Among the solvents tested, high boiling polar solvents (DMSO and DMF) were found more suitable than their low boiling counterpart (EtOH) (Entries 1–14, Table 1). Solvents like CH_3CN and $HOCH_2CH_2NH_2$ were found unsuitable for the purpose (Entries 15–18, Table 1). When the reaction was carried out in the absence of solvent using the liquid substrate, i.e. CH_3NO_2 in excess, significant increase in yields were observed (Entries 19–24, Table 1). To check the role of $CuFe_2O_4$, the reaction was carried out in its absence (Entries 25–26, Table 1). These reactions resulted no and 12% product formation under conventional heating and microwave irradiation respectively and thus revealed the worth of $CuFe_2O_4$ as catalyst in the reaction. 5% catalyst loading was observed as optimal when the isolated yields of the reactions carried out with different catalyst loading were compared (Entry 20, 22 & 24, Table 1). Catalytic effect of Cu(I) and Cu(II)-salts against $CuFe_2O_4$ were checked by carrying out reactions in presence of 5 mol% of Cu $(NO_3)_2$, CuCl, and $CuCl_2$. It was observed that Cu(II) salts display higher catalytic activity than

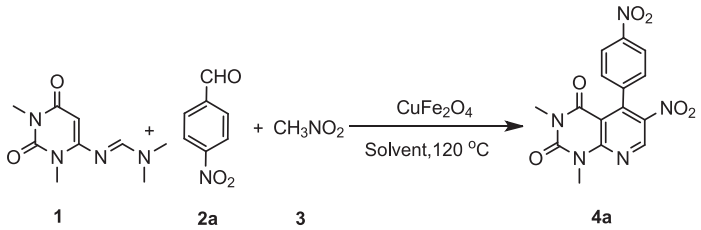

SCHEME 2 Model reaction for the synthesis of 1,3-dimethyl-6-nitro-5-arylpyrido[2,3-*d*]pyrimidine-2,4(1*H*,3*H*)-dione

TABLE 1 Optimization of reaction condition for Scheme 1[a]

Entry	Solvent	Catalyst loading [mol%]	Mode of activation	Yield [%][b]
1	DMSO	10	Conventional heating	20
2			Microwave heating	52
3		5	Conventional heating	18
4			Microwave heating	48
5		3	Conventional heating	15
6			Microwave heating	42
7		—[c]	Conventional heating	—[d]
8			Microwave heating	10
9	DMF	10	Conventional heating	18
10			Microwave heating	45
11		5	Conventional heating	18
12			Microwave heating	40
13	EtOH	10	Conventional heating	—
14			Microwave heating	12
15	CH_3CN	10	Conventional heating	—
16			Microwave heating	—
17	$HOCH_2CH_2NH_2$	10	Conventional heating	—
18			Microwave heating	—
19	—[e]	10	Conventional heating	30
20			Microwave heating	86
21		5	Conventional heating	20
22			Microwave heating	85
23		3	Conventional heating	12
24			Microwave heating	72
25		—	Conventional heating	—
26			Microwave heating	12
27	—	5[f]	Microwave heating	60
28	—	5[g]	Microwave heating	32
29	—	5[h]	Microwave heating	65

[a]Reaction condition: **1** (1 mmol); **2** (1.1 mmol); nitromethane (1.1 mmol); solvent (1 ml/mmol); 12 h (conventional heating); 5 min (microwave heating, 420 W).
[b]Isolated yield of **4a**.
[c]No catalyst.
[d]No **4a** formation.
[e]No solvent, CH_3NO_2 was used in excess (1.5 mmol).
[f]5 mol% of Cu $(NO_3)_2$ was used.
[g]5 mol% of CuCl was used.
[h]5 mol% of $CuCl_2$ was used.

Cu(I) (Entries 27, 28, and 29, Table 1). However, in all the cases, isolated yield of **4a** were found significantly lower than the isolated yields obtained in the presence of $CuFe_2O_4$ as catalyst. Optimization of microwave power employed and amount of nitromethane used were then fine-tuned, the results of which are displayed in Table 2. Increase in microwave power to 480 W (Entry 2, Table 2) resulted no significant change in isolated yield of **4a**, whereas a further increase in that to 540 W (Entry 3, Table 2) caused damage to the reaction mixture resulting lower yield of **4a**. Lowering of microwave energy (Entries 4 and 5, Table 2) led to significant decrease in product formation. Entries 1 and 6–8 of Table 2 demonstrate the effect of amount of nitromethane used on product formation. The use of 1.5 equivalent of nitromethane with respect to 1 equivalent of **1** was found sufficient to fulfill its dual role of substrate and solvent (Entry 1, Table 2). Effect of the period of microwave exposure was finally studied by carrying out the reactions for different time intervals (Entries 1 and 9–11, Table 1) and a reaction time of 5 min was found to be optimal. So a microwave irradiation of 420 W for a period of 5 min and use of 1.5 equivalents of CH_3NO_2 were considered optimal for the work.

To check the generality of our developed methodology for the synthesis of **4**, a series of aromatic aldehydes were tested and the results are summarized in Table 3. From Table 3, it is very clear that the developed methodology is suitable for a wide spectrum of aromatic aldehydes bearing substituents of varied electronic nature at different positions. Although a general conclusion is difficult to draw, however, the presence of electron withdrawing —Cl group at *ortho*-position and strongly electron donating —NMe_2 group at *para*-position of aromatic aldehydes are observed to result decrease in yield (**4h** and **4k**). Although heteroaryl aldehydes also sustain the reaction condition, yields are found to be slightly in lower side (**4f** and **4l**). Attempts were made to carry out the reaction with aliphatic aldehydes (Ethanal and *n*-pentanal) but went in vain.

2.3 | Reaction mechanism

To have some idea about how the reaction progresses, some controlled experiments were carried out under our optimized reaction condition as depicted in Scheme 3. Initially, we carried out a reaction between *p*-nitrobenzaldehyde (**2a**) and nitromethane which resulted (*E*)-1-nitro-4-(2-nitrovinyl)benzene (**5a**) in almost quantitative yield in 2 min (**Reaction 1**). (*E*)-1-nitro-4-(2-nitrovinyl)benzene (**5a**) obtained was purified by recrystallization from EtOH to exclude the excess CH_3NO_2. Pure **5a** obtained was then treated with **1** in a solid phase reaction, and to our delight, the reaction resulted 1,3-dimethyl-6-nitro-5-(4-nitrophenyl)pyrido[2,3-*d*]pyrimidine-2,4(1*H*,3*H*)-dione (**4a**) as product in 60% yield within 3 min (**Reaction 2**). This observation suggested possible involvement of **5a** as intermediate in the reaction. When the reaction was shifted from solid phase to solution phase (using CH_3NO_2 as solvent), a significant increase in product yield (90%) was observed (**Reaction 3**). This can be attributed to uniform mixing of the starting materials in solution phase. In a different attempt, a one pot two step reaction was carried out wherein **1** was directly added to the product mixture of

TABLE 2 Optimization of microwave power and amount of nitromethane for Scheme 1[a]

Entry	Equivalent of CH_3NO_2	Microwave power	Time (min)	Yield [%][b]
1	1.5	420 W	5	85
2	1.5	480 W	5	86
3	1.5	540 W	5	45[c]
4	1.5	350 W	5	72
5	1.5	240 W	5	30
6	1	420 W	5	62
7	2	420 W	5	85
8	3	420 W	5	86
9	1.5	420 W	10	84
10	1.5	420 W	3	70
11	1.5	420 W	1	20

[a]Reaction condition: **1** (1 mmol); **2** (1.1 mmol), nitromethane (1–3 mmol); $CuFe_2O_4$ (5 mol%); microwave heating (350–540 W).
[b]Isolated yield of **4a**.
[c]Reaction mixture got burnt.

TABLE 3 Substrate study of aromatic aldehydes in synthesis of 1,3-dimethyl-6-nitro-5-arylpyrido[2,3-*d*]pyrimidine-2,4(1*H*,3*H*)-diones

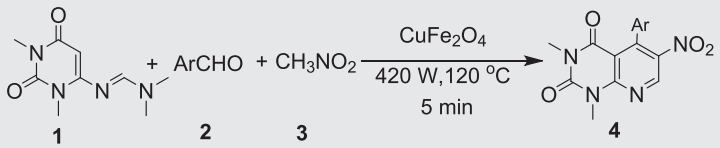

1 2 3 4

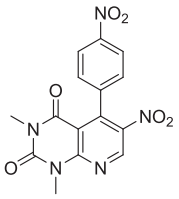

4a (85%)

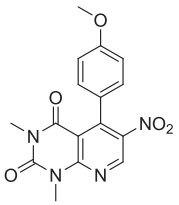

4b (85%)

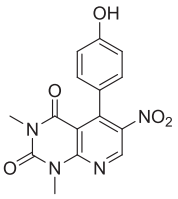

4c (80%)

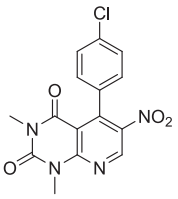

4d (82%)

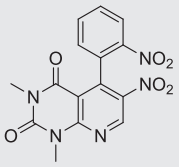

4e (84%)

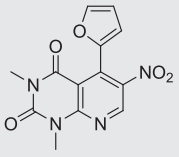

4f, (70%)

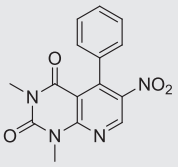

4g (75%)

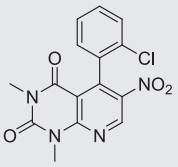

4h (70%)

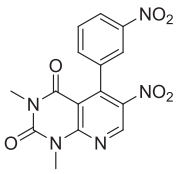

4i (82%)

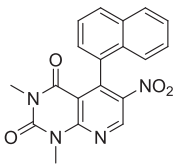

4j (80%)

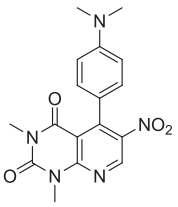

4k (55%)

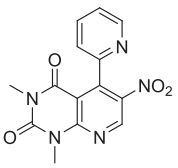

4l (70%)

Note: Stoichiometry of reaction: **1** (1 mmol); **2** (1.1 mmol); **3** (1.5 mmol); $CuFe_2O_4$ (5 mol%). Figures in parenthesis describe isolated yields.

2a and CH_3NO_2 (**3**) of the first step, and the reaction mixture obtained was exposed to MWI (420 W) for 3 min (**Reaction 4**). This resulted to a final product (**4a**) in 80% yield, which is in good agreement with the earlier observations and to the fact that the reaction proceeds via initial formation of **5a**, which then reacts with the third reaction partner, i.e. **1** to furnish the final product (**4a**) in a cascade manner. **Reaction 1** and **Reaction 3** were checked in absence of $CuFe_2O_4$ too as in **Reaction 5** and **Reaction 6**, which resulted their corresponding products in 20% and 45% yields. These results clearly reveal active participation of $CuFe_2O_4$ as catalyst in both the steps of the developed cascade process. Reaction of **1** with **2a** resulted a stable bisuracil derivative (**6**) as product (**Reaction 7**)[58] ruling out the initial reaction between those two in the developed reaction protocol. Further mechanistic studies were not carried out; however, a plausible sequence of reactions for the overall cascade synthetic process is depicted in Scheme 4 based on the observations of the controlled experiments. (*E*)-1-nitro-4-(2-nitrovinyl)benzene (**5a**) formed initially is assumed to undergo Diels-Alder cycloaddition with **1** in a cascade process to result the fused bicyclic product (**7a**), which eliminates one molecule of Me_2NH, followed by aerial aromatization to generate the final product (**4a**).

SCHEME 3 Controlled experiments for Scheme 1

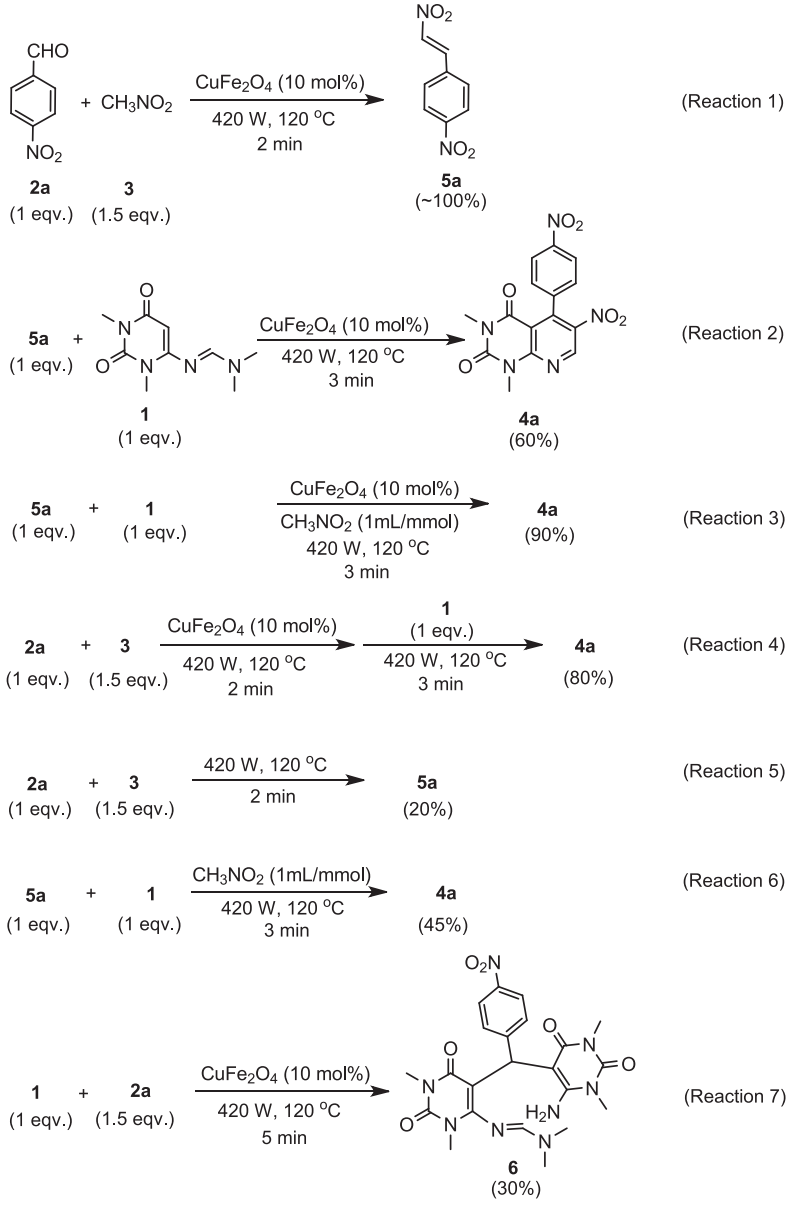

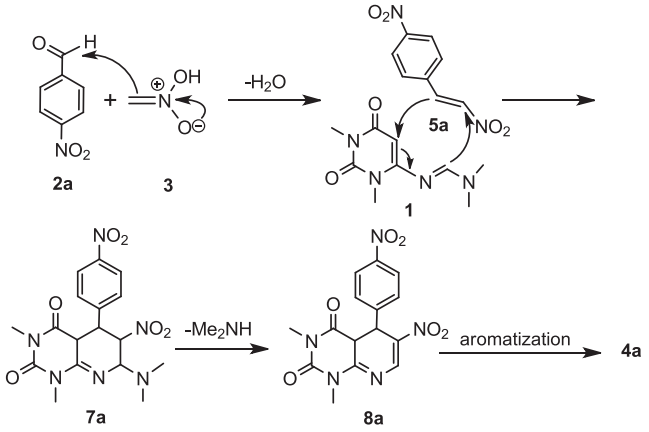

SCHEME 4 Plausible sequence of reactions for cascade synthesis of**4a**

A hot filtration test was conducted to investigate the heterogeneous nature of the catalyst. For this, the reaction was stopped halfway (2 min) under an otherwise optimized reaction condition (reaction condition of Table 3). The catalyst particles were first removed from the hot reaction mixture using a bar magnet and then the reaction mixture was exposed to the reaction condition again for 3 min. Reaction did not proceed after the removal of the catalyst, which reveals the heterogeneous nature of the catalyst. However, AAS analysis of the final reaction mixture detected very small amount of Cu and Fe (4 and 2 ppm, respectively) in it. These two results led us to have the opinion that a very small amount of the magnetically active $CuFe_2O_4$ catalyst underwent some changes under the reaction condition to produce some

substances, which were both magnetically as well as catalytically inactive.

2.4 | Reusability of the catalyst

To check the reusability of the catalyst, a reaction was carried out in gram scale taking **1** (2.1 g, 10 mmol), *p*-nitrobenzaldehyde (1.66 g, 11 mmol), nitromethane (915 mg, 15 mmol), and $CuFe_2O_4$ (430.5 mg, 1.8 mmol) under MWI (420 W) at 120°C. After 5 min, the reaction was stopped, allowed to cool, and recovered the catalyst using a bar magnet. The recovered catalyst was washed thrice with ethanol followed by water and then dried in a hot air oven at 80°C (12 h). Recovered catalyst obtained was used for the subsequent batch of reactions and the product yield obtained are summarized in Figure 7. A slight decrease in activity of the catalyst was observed in every subsequent batch of reactions up to the fourth run of reusing the catalyst, beyond which reusability was not continued. It was observed that while carrying out the hot filtration test, a small fraction of the catalyst might undergo some changes under the reaction condition to produce catalytically and magnetically inactive substances. So slightly reduced amounts of the catalyst were recovered in every subsequent batches of reactions, which can attribute slight decreases in isolated yields of the product in subsequent batches of reaction. The recovered catalyst after fourth run was subjected to SEM-EDX, IR, XRD, and VSM analyses. Although SEM image and XRD data (Figure 1a,b and Figure 3) revealed minor changes in morphology and crystallinity of the catalyst material, SEM-EDX analysis (Figure 1d) ascertained presence of Cu, Fe, and O in the sample. Only a slight shifting of the Fe—O stretching band to lower wave number was observed in the IR spectrum (Figure 2) of the recovered catalyst (576.25 cm^{-1}). VSM study revealed that there was no loss in magnetic property of the catalyst during the catalytic process as the coercivity, magnetization at saturation (Ms), and retentivity (Mr) value of the recovered catalyst sample were found as 259.01 Oe, 34.641 emu/g, and 9.1327 emu/g, respectively (Figure 5).

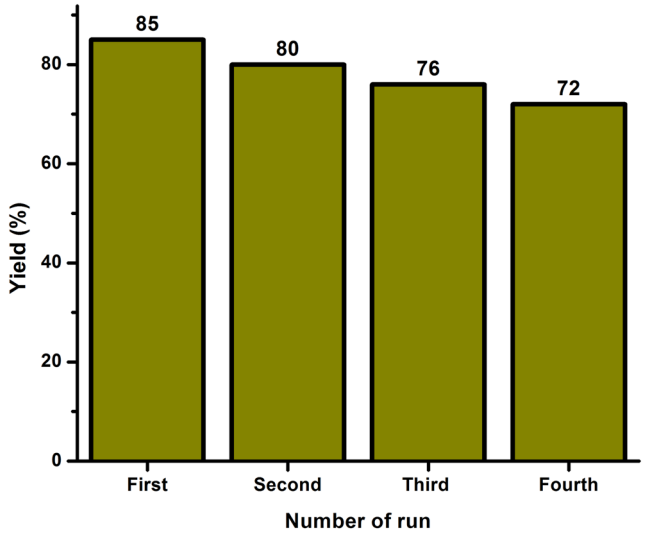

FIGURE 7 Reusability of $CuFe_2O_4$in synthesizing**4a**

3 | EXPERIMENTAL

Chemicals needed were of analytical reagent grade (AR grade) and were used as purchased without further purification. Reactions were carried out using Raga's Scientific Microwave Synthesis System (Model: RG34L). IR spectra were recorded as KBr pallets with a Nicolet iS5 FT-IR spectrophotometer with frequencies expressed in wave numbers (cm^{-1}). ^1H and ^{13}C NMR spectra were recorded with a JNM ECS 400 MHz NMR spectrophotometer (JEOL) using tetramethylsilane (TMS) as the internal standard. Chemical shift values are expressed in ppm. Reactions were monitored by thin-layer chromatography using aluminum sheets with silica gel60F254 (Merck). Ethyl acetate and hexane mixtures at different ratio were used as the mobile phase for separation of the reaction mixture. UV light was used as visualizer. Mass spectrometric analysis were performed using an Agilent Technologies 6520 Accurate-Mass Q-TOF LC mass spectrometer.

3.1 | Preparation of $CuFe_2O_4$ nanoparticles

$CuFe_2O_4$ catalyst was prepared following a procedure as describe in our recent work.[53] Specifically, to a solution of Fe $(NO_3)_2{\cdot}9H_2O$ (3.34 g, 8.2 mmol) and Cu $(NO_3)_2{\cdot}3H_2O$ (1 g, 4.1 mmol) in 75 ml of distilled water, 3 g (75 mmol) of NaOH dissolved in 15 ml of water was added from a dropping funnel at room temperature over a period of 10 min. The reaction mixture was then exposed to ultrasonic irradiation in an ultra-sonication bath preheated at 90°C with occasional stirring. After 2 h, it was cooled to room temperature, and the $CuFe_2O_4$ particles obtained were collected by ultracentrifuge technique, washed with water till complete removal of NaOH, and then kept in an oven for overnight (12 h) at 80°C. The material obtained was grounded in a mortar-pestle, kept in a furnace at 700°C for 5 h, and then allowed to cool to room temperature inside the furnace which finally furnished 780 mg of magnetically active $CuFe_2O_4$ nanoparticles.

3.2 | Representative procedure for the synthesis of 5-arylpyrido[2,3-*d*]pyrimidine

1 (210.2 mg, 1 mmol), *p*-nitrobenzaldehyde aldehyde (166.2 mg, 1.1 mmol), CH_3NO_2 (91.6 mg, 1.5 mmol), and $CuFe_2O_4$ (43.05 mg, 0.18 mmol, 5 mol%) were taken in a 25 ml round bottomed flask and uniformly mixed under stirring. The reaction mixture obtained was then exposed to microwave irradiation (420 W) for 5 min. $CuFe_2O_4$ particles were then recovered using a bar magnet. The residue was dissolved in ethyl acetate (5 ml) and washed with water (5 ml) and brine (5 ml). The organic layer was then dried over anhydrous Na_2SO_4. The crude product was obtained by evaporating the ethyl acetate and then purified by column chromatography using silica gel (100–200 mesh) as adsorbent and ethyl acetate-hexane as eluent.

3.3 | Spectral data of synthesized compounds

3.3.1 | 1,3-Dimethyl-6-nitro-5-(4-nitrophenyl)pyrido[2,3-*d*]pyrimidine-2,4(1*H*,3*H*)-dione (4a)

^{1}H NMR (400 MHz, DMSO): δ = 9.32(s, 1H), 7.49 (d, J = 8.8 Hz, 2H), 7.25 (d, J = 4.8 Hz, 2H), 3.64 (s, 3H), 3.15 (s, 3H); ^{13}C NMR (400 MHz, DMSO): δ = 159.1, 153.2, 150.5, 148.4, 145.5, 142.2, 133.0, 132.5, 108.3, 39.5, 30.4, 28.5. HRMS (ESI-TOF) m/z: $[M + H]^+$. Calcd for $C_{15}H_{11}N_5O_6$ 358.0709; found 358.0708.

3.3.2 | 5-(4-Methoxyphenyl)-1,3-dimethyl-6-nitropyrido[2,3-*d*]pyrimidine-2,4(1*H*,3*H*)-dione (4b)

^{1}H NMR (400 MHz, DMSO): δ = 9.23 (s, 1H), 7.13 (d, J = 8.4 Hz, 2H), 6.97 (d, J = 8.4 Hz, 2H), 3.81 (s, 3H), 3.63 (s, 3H), 3.16 (s, 3H); ^{13}C NMR (400 MHz, DMSO): δ = 159.3, 159.0, 152.9, 150.4, 147.6, 146.4, 143.4, 128.8, 125.0, 113.3, 108.4, 55.1, 30.3, 28.3. HRMS (ESI-TOF) m/z: $[M + H]^+$. Calcd for $C_{16}H_{14}N_4O_5$ 343.0964; found 343.0965.

3.3.3 | 5-(4-Hydroxyphenyl)-1,3-dimethyl-6-nitropyrido[2,3-*d*]pyrimidine-2,4(1*H*,3*H*)-dione (4c)

^{1}H NMR (400 MHz, DMSO): δ = 9.67 (s, 1H), 9.20 (s, 1H), 6.99 (d, J = 8.4 Hz, 2H), 6.78 (d, J = 8.4 Hz, 2H), 3.63 (s, 3H), 3.16 (s, 3H); ^{13}C NMR (400 MHz, DMSO): δ = 159.0, 157.7, 152.8, 150.5, 147.4, 146.6, 143.7, 128.7, 123.3, 114.8, 108.4, 30.4, 28.4. HRMS (ESI-TOF) m/z: $[M + H]^+$. Calcd for $C_{15}H_{12}N_4O_5$ 329.0808; found 329.0807.

3.3.4 | 5-(4-Chlorophenyl)-1,3-dimethyl-6-nitropyrido[2,3-*d*]pyrimidine-2,4(1*H*,3*H*)-dione (4d)

^{1}H NMR (400 MHz, DMSO): δ = 9.32 (s, 1H), 7.49 (d, J = 8.8 Hz, 2H), 7.25 (d, J = 8.4 Hz, 2H), 3.65 (s, 3H), 3.15 (s, 3H); ^{13}C NMR (400 MHz, DMSO): δ = 159.0, 153.1, 150.4, 148.3, 145.5, 142.2, 133.0, 132.5, 129.1, 127.9, 108.3, 30.3, 28.4. HRMS (ESI-TOF) m/z: $[M + H]^+$. Calcd for $C_{15}H_{11}ClN_4O_4$ 347.0469; found 347.0468.

3.3.5 | 1,3-Dimethyl-6-nitro-5-(2-nitrophenyl)pyrido[2,3-*d*]pyrimidine-2,4(1*H*,3*H*)-dione (4e)

^{1}H NMR (400 MHz, DMSO): δ = 9.49 (s, 1H), 8.40 (d, J = 8.0 Hz, 1H), 7.83 (t, J = 7.4 Hz, 1H), 7.75 (t, J = 8.4 Hz, 1H), 7.30 (d, J = 6.4 Hz, 1H), 3.67 (s, 3H), 3.11 (s, 3H), ^{13}C NMR (400 MHz, DMSO): δ = 159.4, 153.5, 150.3, 150.0, 146.6, 146.1, 139.7, 134.9, 130.8, 130.0, 128.5, 124.3, 107.5, 30.4, 28.5. HRMS (ESI-TOF) m/z: $[M + H]^+$. Calcd for $C_{15}H_{11}N_5O_6$ 358.0709; found 358.0708.

3.3.6 | 5-(Furan-2-yl)-1,3-dimethyl-6-nitropyrido[2,3-*d*]pyrimidine-2,4(1*H*,3*H*)-dione (4f)

^{1}H NMR (400 MHz, DMSO): δ = 9.28 (s, 1H), 7.89 (s, 1H), 6.73 (d, J = 3.2 Hz, 1H), 6.64 (q, J = 5.2 Hz, 1H), 3.61 (s, 3H), 3.22 (s, 3H), ^{13}C NMR (400 MHz, DMSO): δ = 158.7, 153.4, 150.5, 148.5, 145.1, 142.6, 142.1,134.7, 113.2, 111.8, 108.2, 30.4, 28.5. HRMS (ESI-TOF) m/z: $[M + H]^+$. Calcd for $C_{13}H_{10}N_4O_5$ 303.0651; found 303.0652.

3.3.7 | 1,3-Dimethyl-6-nitro-5-phenylpyrido[2,3-*d*]pyrimidine-2,4(1*H*,3*H*)-dione (4g)

^{1}H NMR (400 MHz, DMSO): δ = 9.27(s, 1H), 7.41 (d, J = 8.0 Hz, 3H), 7.20 (d, J = 8.0 Hz, 2H), 3.64 (s, 3H), 3.14 (s, 3H), ^{13}C NMR (400 MHz, DMSO): δ = 159.0, 153.1, 150.5, 148.0, 146.5, 142.9, 133.3, 128.4, 127.8, 127.2,

108.2, 30.1, 28.2. HRMS (ESI-TOF) m/z: $[M + H]^+$. Calcd for $C_{15}H_{12}N_4O_4$ 313.0859; found 313.0858.

3.3.8 | 5-(2-Chlorophenyl)-1,3-dimethyl-6-nitropyrido[2,3-*d*]pyrimidine-2,4(1*H*,3*H*)-dione (4h)

^{1}H NMR (400 MHz, DMSO): δ = 9.42 (s, 1H), 7.53 (d, J = 8 Hz, 1H), 7.45 (t, J = 7.2 Hz, 1H), 7.38 (t, J = 7.2 Hz, 1H), 7.20 (d, J = 7.2, 1H), 3.66 (s, 3H), 3.16 (s, 3H); ^{13}C NMR (400 MHz, DMSO): δ = 158.8, 153.4, 150.4, 149.3, 144.0, 141.3, 133.0, 131.2, 130.0, 128.6, 128.3, 127.0, 108.2, 30.4, 28.4. HRMS (ESI-TOF) m/z: $[M + H]^+$. Calcd for $C_{15}H_{11}ClN_4O_4$ 347.0469; found 347.0468.

3.3.9 | 1,3-Dimethyl-6-nitro-5-(3-nitrophenyl)pyrido[2,3-*d*]pyrimidine-2,4(1*H*,3*H*)-dione (4i)

^{1}H NMR (400 MHz, DMSO): δ = 9.42 (s, 1H), 8.32–8.20 (m, 2H), 7.77–7.71 (m, 2H), 3.67 (s, 3H), 3.14 (s, 3H), ^{13}C NMR (400 MHz, DMSO): δ = 159.2, 153.4, 150.5, 149.2, 147.3, 144.5, 141.4, 135.9, 134.0, 129.6, 123.1, 122.3, 108.5, 30.4, 28.4. HRMS (ESI-TOF) m/z: $[M + H]^+$. Calcd for $C_{15}H_{11}N_5O_6$ 358.0709; found 358.0708.

3.3.10 | 1,3-Dimethyl-5-(naphthalen-1-yl)-6-nitropyrido[2,3-*d*]pyrimidine-2,4(1*H*,3*H*)-dione (4j)

^{1}H NMR (400 MHz, DMSO): δ = 9.40(s, 1H), 7.98 (t, 2H), 7.51 (t, 2H), 7.41–7.35 (m, 2H), 7.23 (d, 1H), 3.69 (s, 3H), 3.05 (s, 3H); ^{13}C NMR (400 MHz, DMSO): δ = 158.8, 153.5, 150.7, 148.8, 145.6, 143.0, 132.6, 131.2, 128.6, 128.3, 126.5, 126.1, 125.3, 125.0, 124.1, 109.4, 30.4, 28.3. HRMS (ESI-TOF) m/z: $[M + H]^+$. Calcd for $C_{19}H_{14}N_4O_4$363.1015; found 363.1016.

3.3.11 | 5-(4-(Dimethylamino)phenyl)-1,3-dimethyl-6-nitropyrido[2,3-*d*]pyrimidine-2,4(1*H*,3*H*)-dione (4k)

^{1}H NMR (400 MHz, DMSO): δ = 9.15 (s, 1H), 7.01 (d, J = 8.4 Hz, 2H), 6.71 (d, J = 8.8 Hz, 2H), 3.62 (s, 3H), 3.16 (s, 3H), 2.97 (s, 6H); ^{13}C NMR (400 MHz, DMSO): δ = 159.13, 152.97, 150.60, 147.17, 146.82, 143.83, 128.61, 119.57, 111.14, 108.31, 30.62, 29.01, 28.28. HRMS (ESI-TOF) m/z: $[M + H]^+$. Calcd for $C_{17}H_{17}N_5O_4$ 356.1281; found 356.1282.

3.3.12 | 1,3-Dimethyl-6-nitro-5-(pyridin-2-yl)pyrido[2,3-*d*]pyrimidine-2,4(1*H*,3*H*)-dione (4l)

^{1}H NMR (400 MHz, DMSO): δ = 9.32 (s, 1H), 8.49 (d, J = 4.8 Hz, 1H), 7.85 (t, J = 7.6/9.2 Hz, 1H), 7.43 (t, J = 7.6 Hz, 2H), 3.62 (s, 3H), 3.11 (s, 3H); ^{13}C NMR (400 MHz, DMSO): δ = 159.86, 154.17, 153.43, 151.48, 150.28, 149.22, 145.97, 141.48, 136.98, 124.60, 124.13, 108.46, 31.18, 29.21. HRMS (ESI-TOF) m/z: $[M + H]^+$. Calcd for $C_{14}H_{11}N_5O_4$ 314.0381; found 314.0380.

4 | CONCLUSIONS

In conclusion, we have developed an efficient methodology for the synthesis of 1,3-dimethyl-6-nitro-5-arylpyrido[2,3-*d*]pyrimidine-2,4(1*H*,3*H*)-diones starting from 6-[(dimethylamino)methylene-amino]-1,3-dimethyluracil, aromatic aldehydes, and nitromethane under microwave irradiation in solvent less condition. A salient feature of the current methodology is its cascade nature, which makes it step-economic avoiding isolation of the intermediate. The methodology demonstrates the first use of heterogeneous catalyst ($CuFe_2O_4$) in multicomponent synthesis of 5-arylpyrido[2,3-*d*]pyrimidine involving 6-[(dimethylamino)methylene-amino]-1,3-dimethyluracil as one of the substrates. It enjoys the advantage of being significantly time economic over other existing procedures. Easy recovery and good reusability of the catalyst, simple operating procedure, wide substrate scope, good to excellent product yield, and so forth ensure it to be a methodology to go for the synthesis of 1,3-dimethyl-6-nitro-5-arylpyrido[2,3-*d*]pyrimidine-2,4(1*H*,3*H*)-diones.

FUNDING

P. B. and L. S. are indebted to the Department of Science and Technology-Science and Engineering Research Board, India, for financial support to the project (EMR/2016/003126). L. S. is also grateful to Council of Scientific and Industrial Research (CSIR), India for financial support through project (02(0280)/16/EMR-II). A. J. B. is a receiver of DST-INSPIRE fellowship (IF170498) and is grateful to DST for the same.

ACKNOWLEDGMENTS

Authors acknowledge MHR research group of the Department of Chemistry, Rajiv Gandhi University for giving access to the ultrasonicator. Analytical support from SAIC, Tezpur University is gratefully acknowledged.

AUTHOR CONTRIBUTIONS

Amar Bhuyan: Methodology. **Pubanita Bhuyan:** Conceptualization. **Dr. Bornali Boruah:** Resources. **LAKHINATH SAIKIA:** Conceptualization; resources; supervision.

ORCID

Amar Jyoti Bhuyan https://orcid.org/0000-0002-4963-4974
Pubanita Bhuyan https://orcid.org/0000-0003-3131-4611
Bornali Boruah https://orcid.org/0000-0001-8790-662X
Lakhinath Saikia https://orcid.org/0000-0003-0252-2120

REFERENCES

[1] C. Kurumurthy, P. Sambasiva Rao, B. Veera swamy, G. Santhosh kumar, P. Shanthan Rao, B. Narsaiah, L. R. Velatooru, R. Pamanji, J. Venkateswara Rao, *Eur. J. Med. Chem.* **2011**, *46*, 3462.
[2] M. M. Gineinah, M. N. A. Nasr, S. M. I. Badr, W. M. El-Husseiny, *Med. Chem. Res.* **2013**, *22*, 3943.
[3] A. Gangjee, O. Adair, S. F. Queener, *J. Med. Chem.* **1999**, *42*, 2447.
[4] H. B. El-Nassan, *Eur. J. Med. Chem.* **2011**, *46*, 2031.
[5] O. A. Abdelaziz, W. M. El Husseiny, K. B. Selim, H. M. Eisa, *Bioorg. Chem.* **2019**, *90*, 103076.
[6] S. Ravi Kanth, G. Venkat Reddy, K. Hara Kishore, P. Shanthan Rao, B. Narsaiah, U. Surya Narayana Murthy, *Eur. J. Med. Chem.* **2006**, *41*, 1011.
[7] B. Lakshmi Narayana, A. Raghu Ram Rao, P. Shanthan Rao, *Eur. J. Med. Chem.* **2009**, *44*, 1369.
[8] A. Bazgir, M. M. Khanaposhtani, A. A. Soorki, *Bioorg. Med. Chem. Lett.* **2008**, *18*, 5800.
[9] M. Fares, S. R. Abd El Hadi, R. A. Eladwy, A. A. Shoun, M. M. Abdel-Aziz, W. M. Eldehna, H. A. Abdel-Aziz, P. A. Keller, *Org. Biomol. Chem.* **2018**, *16*, 3389.
[10] J. Matsumoto, S. Minami, *J. Med. Chem.* **1975**, *18*, 74.
[11] B. Veeraswamy, D. Madhu, G. Jitender Dev, Y. Poornachandra, G. Shravan Kumar, C. Ganesh Kumar, B. Narsaiah, *Bioorg. Med. Chem. Lett.* **2018**, *28*, 1670.
[12] H. Huang, D. A. Hutta, J. M. Rinker, H. Hu, W. H. Parsons, C. Schubert, R. L. DesJarlais, C. S. Crysler, M. A. Chaikin, R. R. Donatelli, Y. Chen, D. Cheng, Z. Zhou, E. Yurkow, C. L. Manthey, M. R. Player, *J. Med. Chem.* **2009**, *52*, 1081.
[13] A.-R. B. A. El-Gazzar, H. N. Hafez, *Bioorg. Med. Chem. Lett.* **2009**, *19*, 3392.
[14] D.-W. Wang, Q. Li, K. Wen, I. Ismail, D.-D. Liu, C.-W. Niu, X. Wen, G.-F. Yang, Z. Xi, *J. Agric. Food Chem.* **2017**, *65*, 5278.
[15] J. F. Dorsey, R. Jove, A. J. Kraker, J. Wu, *Cancer Res.* **2000**, *60*, 3127.
[16] N. Kammasud, C. Boonyarat, K. Sanphanya, M. Utsintong, S. Tsunoda, H. Sakurai, I. Saiki, I. André, D. S. Grierson, O. Vajragupta, *Bioorg. Med. Chem. Lett.* **2009**, *19*, 745.
[17] C. J. C. Connolly, J. M. Hamby, M. C. Schroeder, M. Barvian, G. H. Lu, R. L. Panek, A. Amar, C. Shen, A. J. Kraker, D. W. Fry, W. D. Klohs, A. M. Doherty, *Bioorg. Med. Chem. Lett.* **1997**, *7*, 2415.
[18] M. T. El Sayed, H. A. R. Hussein, N. M. Elebiary, G. S. Hassan, S. M. Elmessery, A. R. Elsheakh, M. Nayel, H. A. Abdel-Aziz, *Bioorg. Chem.* **2018**, *78*, 312.
[19] V. Nair, G. Chi, Q. Shu, J. Julander, D. F. Smee, *Bioorg. Med. Chem. Lett.* **2009**, *19*, 1425.
[20] J. R. Miller, S. Dunham, I. Mochalkin, C. Banotai, M. Bowman, S. Buist, B. Dunkle, D. Hanna, H. J. Harwood, M. D. Huband, A. Karnovsky, M. Kuhn, C. Limberakis, J. Y. Liu, S. Mehrens, W. T. Mueller, L. Narasimhan, A. Ogden, J. Ohren, J. V. N. V. Prasad, J. A. Shelly, L. Skerlos, M. Sulavik, V. H. Thomas, S. VanderRoest, L. Wang, Z. Wang, A. Whitton, T. Zhu, C. K. Stover, *PNAS* **2009**, *106*, 1737.
[21] M. M. Sarmah, D. Prajapati, *RSC Adv.* **2014**, *4*, 22955.
[22] S. Das, A. J. Thakur, T. Medhi, B. Das, *RSC Adv.* **2013**, *3*, 3407.
[23] R. Sarma, K. J. Borah, Y. Dommaraju, D. Prajapati, *Mol. Diversity* **2011**, *15*, 697.
[24] D. Prajapati, M. Sarmah, W. Hu, *Synlett* **2013**, *24*, 471.
[25] D. Prajapati, M. Gohain, B. J. Gogoi, J. S. Sandhu, *Synlett* **2004**, 1179. https://doi.org/10.1055/s-2004-825601
[26] P. Saikia, A. J. Thakur, D. Prajapati, J. S. Sandhu, *Indian J. Chem.* **2002**, *41B*, 804.
[27] A. J. Thakur, P. Saikia, D. Prajapati, J. S. Sandhu, *Synlett* **2001**, *8*, 1299.
[28] E. B. Walsh, Z. Nai-Jue, G. Fang, H. Wamhoff, *Tetrahedron Lett.* **1988**, *29*, 4401.
[29] M. Daraie, M. M. Heravi, M. Mirzaei, N. Lotfian, *Appl. Organomet. Chem.* **2019**, *33*, e5058.
[30] B. Mirhosseini-Eshkevari, M. A. Ghasemzadeh, M. Esnaashari, *Appl. Organomet. Chem.* **2019**, *33*, e5027.
[31] J. Safari, M. Tavakoli, M. A. Ghasemzadeh, *J. Organomet. Chem.* **2019**, *880*, 75.
[32] N. Jamasbi, M. Irankhah-Khanghah, F. Shirini, H. Tajik, M. S. N. Langarudi, *New J. Chem.* **2018**, *42*, 9016.
[33] F. Zhang, C. Li, X. Liang, *Green Chem.* **2018**, *20*, 2057.
[34] S. Moradi, M. A. Zolfigol, M. Zarei, D. A. Alonso, A. Khoshnood, A. Tajally, *Appl. Organomet. Chem.* **2018**, *32*, e4043.
[35] M. Mohsenimehr, M. Mamaghani, F. Shirini, M. Sheykhan, F. A. Moghaddam, *Chin. Chem. Lett.* **2014**, *25*, 1387.
[36] S. P. Satasia, P. N. Kalaria, D. K. Raval, *Org. Biomol. Chem.* **2014**, *12*, 1751.
[37] F. Nemati, R. Saeedirad, *Chin. Chem. Lett.* **2013**, *24*, 370.
[38] S. Abdolmohammadi, M. Afsharpour, *Chin. Chem. Lett.* **2012**, *23*, 257.
[39] K. Nurjamal, G. Brahmachari, *ChemistrySelect* **2019**, *4*, 2363.
[40] R. Aryan, H. Beyzaei, M. Nojavan, F. Pirani, H. Samareh Delarami, M. Sanchooli, *Mol. Diversity* **2019**, *23*, 93.
[41] P. Acosta, B. Insuasty, R. Abonia, M. Gutierrez, J. Quiroga, *Mol. Diversity* **2017**, *21*, 943.
[42] O. G. Jolodar, F. Shirini, M. Seddighi, *Chin. J. Catal.* **2017**, *38*, 1245.
[43] A. Upadhyay, L. K. Sharma, V. K. Singh, R. K. P. Singh, *Tetrahedron Lett.* **2016**, *57*, 5599.
[44] S. Singh, M. Saquib, M. Singh, J. Tiwari, F. Tufail, J. Singh, J. Singh, *New J. Chem.* **2016**, *40*, 63.
[45] F. Belhadj, Z. Kibou, N. Cheikh, N. Choukchou-Braham, D. Villemin, *Tetrahedron Lett.* **2015**, *56*, 5999.

[46] M. Jatczak, K. Muylaert, L. M. De Coen, J. Keemink, B. Wuyts, P. Augustijns, C. V. Stevens, *Bioorg. Med. Chem.* **2014**, *22*, 3947.
[47] A. Gangjee, O. A. Namjoshi, S. Raghavan, S. F. Queener, R. L. Kisliuk, V. Cody, *J. Med. Chem.* **2013**, *56*, 4422.
[48] S. Paul, G. Pal, A. R. Das, *RSC Adv.* **2013**, *3*, 8637.
[49] A. S. Kumar, M. A. Reddy, M. Knorn, O. Reiser, B. Sreedhar, *Eur. J. Org. Chem.* **2013**, *2013*, 4674.
[50] K. B. Rasal, G. D. Yadav, *Catal. Today* **2018**, *309*, 51.
[51] B. Sreedhar, A. S. Kumar, D. Yada, *Tetrahedron Lett.* **2011**, *52*, 3565.
[52] A. Dandia, A. K. Jain, S. Sharma, *RSC Adv.* **2013**, *3*, 2924.
[53] P. Bhuyan, P. Bhorali, I. Islam, A. J. Bhuyan, L. Saikia, *Tetrahedron Lett.* **2018**, *59*, 1587.
[54] I. Nedkov, R. E. Vandenberghe, T. Marinova, P. Thailhades, T. Merodiiska, I. Avramova, *Appl. Surf. Sci.* **2006**, *253*, 2589.
[55] Y. Zhao, G. He, W. Dai, H. Chen, *Ind. Eng. Chem.* **2014**, *53*, 12566.
[56] S. Vepřek, D. L. Cocke, S. Kehl, H. R. Oswald, *J. Catal.* **1986**, *100*, 250.
[57] M. Zhu, D. Meng, C. Wang, G. Diao, *ACS Appl. Mater. Interfaces* **2013**, *5*, 6030.
[58] S. Das, S. J. Kalita, P. Bharali, B. K. Konwar, B. Das, A. J. Thakur, *ACS Sustainable Chem. Eng.* **2013**, *1*, 1530.

SUPPORTING INFORMATION

Additional supporting information may be found online in the Supporting Information section at the end of this article.

How to cite this article: Bhuyan AJ, Bhuyan P, Boruah B, Saikia L. Magnetically recoverable copper ferrite catalyzed cascade synthesis of 1,3-dimethyl-6-nitro-5-arylpyrido[2,3-*d*]pyrimidine-2,4(1*H*,3*H*)-diones under microwave irradiation and solvent-less condition. *Appl Organomet Chem*. 2020;e6091. https://doi.org/10.1002/aoc.6091